L-MEB: A simple model at L-band for the continental areas - Application to the simulation of a half-degree resolution and global scale data set.

Jean-Pierre Wigneron, Jean-Christophe Calvet, Patricia De Rosnay, Yann Kerr

L-MEB: A simple model at L-band for the continental areas - Application to the simulation of a half-degree resolution and global scale data set.

Jean-Pierre Wigneron, INRA EPHYSE, wigneron@bordeaux.inra.fr

T. Pellarin, CESBIO Toulouse, thierry.pellarin@cesbio.cnes.fr
Jean-Christophe Calvet, METEO-FRANCE/CNRM, calvet@meteo.fr
Patricia de Rosnay, CESBIO Toulouse, patricia.derosnay@cesbio.cnes.fr
Kerr, CESBIO Toulouse, yann.kerr@cesbio.cnes.fr

1. Introduction

L-band (1-2 GHz) microwave radiometry is the most relevant remote sensing technique to monitor soil moisture over land surfaces at the global scale. A synthetic multi-angular brightness temperature data set over land surfaces was simulated at 1.4 GHz, at a half-degree resolution and at the global scale (Pellarin et al., 2003a). This data set was built in order to develop and validate methods to retrieve soil moisture for near-future 1.4 GHz space missions.

Brightness temperatures were computed using a simple model (L-MEB, L-band Microwave Emission of the Biosphere) based on radiative transfer equations. The L-MEB model is the result of an extensive review of the current knowledge of the microwave emission of various land covers (herbaceous and woody vegetation, frozen and unfrozen bare soil, snow, etc.) at L-Band considering that the model should be simple enough to be compatible with the simulation of a half-degree resolution and global scale data set. This model was parameterized for simulating L-band observations (in the 1-2 GHz range) but the model equations remain valid in a low frequency range (about 1 to 10 GHz) and thus including the L-, C- and X-bands.

The soil and vegetation characteristics needed to initialize the L-MEB model were derived from existing land cover maps. Continuous simulations from a land-surface scheme for 1987 and 1988 provided time series of the main variables driving the L-MEB model: soil temperature at the surface and at depth, surface soil moisture, proportion of frozen surface soil moisture, and snow cover characteristics (depth, density, grain size, liquid water content).

The different components of the emission model are described in the following sections. These sections present the general formulation of T_B for a composite pixel and the microwave emission modules for soil, vegetation-covered surfaces, open water, snow-covered surfaces and atmospheric effects.

2. Composite pixel emission

Four main surface types, and the associated values of their cover fraction within each pixel, were considered in the simulations: (i) Bare soil surfaces (ii) Low vegetation canopies (either grassland or crop; mixed grassland/crop landscapes were not considered) (iii) Forest canopies (a distinction was made between tropical, temperate broadleaf and coniferous forests) (iv) Open water surfaces (lakes, rivers, ...).

The brightness temperature of the mixed pixel was written as a linear combination of each cover fraction:

$$Tb_P = f_B\, Tb_{P\text{-}B} + f_F\, Tb_{P\text{-}F} + f_H\, Tb_{P\text{-}H} + f_W\, Tb_{P\text{-}W} \qquad (1)$$

where f_X and $Tb_{p\text{-}X}$ are the cover fraction and the p-polarized brightness temperature of the different surface types (X=B for bare soil, X=F for forests, X=H for herbaceous vegetation-covered surfaces, X=W for open water surfaces). The modeling of $Tb_{P\text{-}X}$ also included the reflection of the down-welling sky radiation by the surface.

Tb_P at the surface level, i.e. as observed immediately above the canopy, is described by (1). As described in the literature (Ulaby et al., 1986) upward atmospheric emission ($Tb_{SKY\text{-}U}$) and atmospheric

attenuation (parameterized by the atmospheric optical thickness τ_{ATM}) had to be taken into account for simulating top-of-the-atmosphere (TOA) T_B:

$$Tb_{p\_SPACE} = Tb_P \exp(-\tau_{ATM}) + Tb_{SKY-U} \quad (2)$$

where $Tb_{P-SPACE}$ is the brightness temperature as seen by a space-borne instrument. A simplified approach was developed in this study to compute τ_{ATM} and Tb_{SKY}.
The modeling of Tb_{P-X} for each kind of surface types (soil, vegetation, water, forest) including the effect of snow and atmosphere is described in the following sections.

3. Soil emission

The bare soil brightness temperature Tb_{SOIL-p} (for polarization p) can be expressed as Ulaby et al. (1986):

$$Tb_{SOIL-p} = e_P T_S^E = (1- r_P) T_S^E \quad (3)$$

where, e_P is the soil microwave emissivity, r_P is the reflectivity at the soil / atmosphere interface, and T_S^E is the soil effective temperature which accounts for the fact that soil emission is originating from a soil layer in which soil temperature generally varies with depth. The soil reflectivity r_P is mainly a function of soil moisture, through the soil dielectric permittivity ε_S, and of surface roughness effects.
Computation of the soil effective temperature (T_S^E) was done following the approach of Wigneron et al. (2001) that accounts for surface soil moisture and which was improved by de Rosnay (see the contribution in this chapter). Modeling of surface roughness effects was based on the semi-empirical approach by Wigneron et al. (2001) and is also described in this chapter.
Only modeling of the soil dielectric permittivity (ε_S) will be described here. This parameter is mainly driven by the soil moisture content but soil textural and structural properties also influence ε_S. Several models have been developed to relate ε_S to soil parameters (soil moisture, bulk density, proportion of sand and clay, etc.) in the lower microwave frequency range (1 – 20 GHz). In L-MEB, the model of Dobson et al. (1985) was used to compute ε_S in the general case. For dry sandy soils, the approach proposed by Mätzler (1998) was used. The Mätzler model accounts for the specific dielectric behavior of dry desert sand: a Debye relaxation model is used to fit experimental measurements in the 1-10 GHz frequency range, and the soil dielectric permittivity ε_S is computed as

$$\varepsilon_S = \varepsilon_\infty + (\varepsilon_0 - \varepsilon_\infty) / (1 - i (f/f_0)) + i a'' \quad (4)$$

where f is frequency, $\varepsilon_0 = 2.79$, $\varepsilon_\infty = 2.53$, $f_0 = 0.27$ GHz, and a''=0.002.
Dry sandy soils were defined in this study as soils with a volumetric soil moisture, w_S, lower than 0.02 m^3/m^3 and a sand fraction higher than 90 %. Note that the use of two different modeling approaches (Dobson et al. and Mätzler) may introduce some discontinuities in the modeling of ε_S. A more general modeling approach of ε_S should be developed to avoid these non-physical discontinuities.
Soil freezing affects ε_S considerably. Measurements of soil dielectric constant at L-band have been obtained by Hallikainen et al. (1984, 1985) in wet, frozen and unfrozen conditions. According to these observations, the real part of ε_S (ε_S') is close to 5 for frozen soils. This value is relatively independent of soil texture, temperature and frequency. For very low temperatures (close to -50 °C) and for specific soil textures, ε_S' may decrease down to 4. The imaginary part of ε_S (ε_S'') of a frozen soil was found to be lower than 1 for most soil types. The values of ε_S'' depend significantly on temperature. For very low soil temperatures (lower than -50 °C), ε_S'' can be close to zero. However, for temperatures between -0.5 and -10 °C, ε_S'' is close to 0.5 for most soil types. Similar conclusions were obtained by Mätzler (personal communication). C. Mätzler noted that for frozen soil (a sandy loam) very constant L-band ε_S values were measured by the PAMIR system. With decreasing temperature this value seems to decrease to about 4 at -6°C to -10°C. The freezing temperature was found to be very close to 0°C and larger than -1°C. Due to ions and salts in the soil there is still some liquid water present in the frozen soil.

As no detailed model is available to parameterize accurately the possible effect of water inclusion in frozen soil on the soil dielectric constant, the permittivity of frozen soil (ε_{SF}) was set equal to a constant:

$$\varepsilon_{SF} = 5 + 0.5i \quad (5)$$

A rapid evaluation of this formula was done. A simple sensitivity study (Figure 1) showed, that if the real part of ε is set equal to 5 (ε'=5), the surface emissivity at both polarization is almost insensitive to variation of the imaginary part of ε in the range (0.01-1). On the contrary, it can be seen that the emissivity is strongly sensitive to the real part of ε (when Re(ε) vary from 4 to 5, an increase in emissivity of about 10K can be seen at H polarization at incidence angle θ =40°C).

In this study, two soil variables describe the status of water within the soil: the volumetric fraction of ice (X_I) and of liquid water (X_M). It was assumed that these fractions were also good descriptors of the frozen and un-frozen soil fractions. Using these variables, a simple mixing model was used to compute the dielectric constant of partially frozen soils (ε_{SP}):

$$\varepsilon_{SP} = X_I/(X_I + X_M)\, \varepsilon_{SF} + X_M/(X_I + X_M)\, \varepsilon_S \quad (6)$$

where ε_{SF} is given by (5), and ε_S is computed using the Dobson et al. or Mätzler models.

Insert Fig. 1

4. Vegetation emission

In the (0.3 GHz - 2 GHz) frequency range, the emission of a vegetation canopy is well described using a simple radiative transfer formulation, hereafter referred to as the τ - ω model (Mo et al., 1982; Brunfeldt et al., 1984; Ulaby et al., 1986). This model is a zero-order solution of the radiative transfer (R.T.) equations as it assumes that the phase matrix term can be neglected (Chanzy and Wigneron, 2000; see also the study by C. Mätzler in this book). Even at L-band (scattering effects are considered to be very low at low frequencies) the elimination of the scattering source term is a strong hypothesis. However, the τ - ω model has usually been found to be an accurate approach to model the L band emission from a vegetation canopy in numerous studies (Mo et al., 1982; Brunfeldt et al., 1984, 1986; Pampaloni et al., 1986; Jackson and Schmugge, 1991; Wigneron et al., 1995; van de Griend et al., 1996) and that it is also a tractable tool for inversion processes (van de Griend et al., 1993; Wigneron et al., 2003). Detailed equations of the τ -ω model are given in the literature (e.g. Ulaby et al., 1986) and will not be reproduced here.

Using this model, the main task was to assign values to the vegetation model parameters (mainly τ and ω) as a function of the vegetation characteristics (canopy type, phenological stage, water content, biomass, etc.)

The vegetation optical thickness τ is generally found to be linearly related to the total vegetation water content VW_C (kg/m^2), using the so-called b parameter (Jackson and Schmugge, 1991):

$$\tau = b\, VWC \quad (7)$$

At 1.4 GHz, a value of b= 0.12 +/-0.03 was found to be representative of most agricultural crops. Numerous authors have investigated the parameterization of b as a function of cover types, temperature and vegetation biomass or water content (see the study by A. Van de Griend and Wigneron in this chapter). For forests, the application of a zero order RT theory is not straightforward, since branch scattering is appreciable even at L-band. However, an equivalent τ -ω formulation was derived by Ferrazzoli et al. (2002) from a detailed analysis of forest microwave signatures at L-band. This formulation is fully described in this book by P. Ferrazzoli. For herbaceous vegetation, VW_C was related to the Leaf Area Index (LAI, m^2/m^2), as indicated in Table II, in order to compute VW_C values from the global LAI estimates given by existing global maps derived from remote sensing observations. An analysis made over agricultural crops showed that the VW_C / LAI ratio is about 0.5 kg/m^2 when the vegetation is well-developed. This value was close to that obtained for herbaceous

vegetation over a fallow (VW_C /LAI ≈ 0.42 kg/m^2 in Fig 2.). A summary of the values of the vegetation parameters used in L-MEB is given in Table 1.

Table 1. L-MEB parameters of the vegetation microwave emission τ -ω model for 2 classes of herbaceous vegetation (grasslands and crops) and 3 classes of woody vegetation (rainforests, deciduous forests, and coniferous forests).

Surface Type	ω	b	VWC (τ = b .VWC)
Grasslands	0.05	0.2	0.5 LAI (kg m^{-2})
Crops	0.05	0.15	0.5 LAI (kg m^{-2})
Rainforests	0.15	0.33	6 kg m^{-2} (branches)
Deciduous forests	0.15	0.33	4 kg m^{-2} (branches)
Coniferous forests	0.15	0.33	3 kg m^{-2} (branches)

Insert Fig. 2

5. The emission of water bodies

It was assumed that the emissivity of calm, unfrozen lakes could be represented by the Fresnel formula (as that used for smooth bare soil) applied with the permittivity of pure water. As no modeling approach could be found in the literature to account for roughness effects (in windy conditions, roughness conditions are very different from those over the ocean), the water bodies were assumed to have a smooth surface. Permittivity of pure ice was used instead of permittivity of saline water for temperatures below -0.5°C.

6. Snow-covered surfaces

The zero-order HUT (Helsinki University of Technology) model, developed by Pulliainen et al. (2001), was used to model snow emission (see study by C. Mätzler in this book). In the presence of vegetation, only two cases were considered in this study: (i) over herbaceous covers, it was assumed that the snow cover overlays the vegetation canopy, (ii) over forest covers, it was assumed that the snow cover overlays the soil surface (the snow located on the forest branches was assumed to be transparent). For snow overlaying herbaceous vegetation canopies, a simple two-step modeling approach was applied:

(1) First, the soil/vegetation emission (T_{B1}) was computed using the τ -ω model.

(2) Second, it was considered that this emission is that of the ground which is overlaid by snow. The HUT model was used to compute the snow cover emission, T_{B1} being substituted to the soil emission.

Using this approach, the continuity of the simulations is maintained when a snow mantel appears or disappears in relation with the climatic conditions. Also, it would be difficult to demonstrate that more complex approaches would be more accurate. If the snow is dry, the total emission is that of the vegetation cover. If the snow is rather wet, the total emission is dominated by the snow layer contribution. For intermediate cases, the total emission is due to the contributions of soil, vegetation and snow. For snow under forest canopies, the snow layer was assumed to overlay the ground, below the trees. A two-step modeling approach quite similar to that used in the case of low canopies was implemented.

These approaches do not really account for the emission by a four-layer medium (in theory, a four-layer medium: soil/vegetation/snow/atmosphere or soil/snow/forest/atmosphere should be considered). However, they are very simple and fit well to global simulations, for which a simplified characterization of the surface variables has to be used.

7. Influence of the atmosphere at L-band

The atmosphere is relatively transparent to L-band microwave radiation. However, atmospheric constituents such as clouds, water vapor or precipitation slightly affect the land surface emission as measured by space-borne observation systems, and TOA brightness temperatures must be corrected for atmospheric effects. From the radiative transfer equations, the down-welling atmospheric emission, $Tb_{SKY\text{-}D}(\theta)$, can be expressed as a function of the atmospheric optical thickness (τ_{ATM}) and the equivalent temperature of the atmosphere (T_{ATMeq}):

$$Tb_{SKY\text{-}D}(\theta) = T_{ATMeq}\,(1 - \exp(-\tau_{ATM}/\cos(\theta))) + T_{csomos}\exp(-\tau_{ATM}/\cos(\theta)) \qquad (8)$$

where T_{cosmos} = 2.7 K. Since these values are relatively little affected by weather, it is expected that a simple parameterization, using commonly available atmospheric variables, may be used instead of a full radiative transfer scheme requiring a lot of input data (radiosoundings, etc.).

A study was carried out using a one-day global numerical weather forecast of the European Centre for Medium-range Weather Forecasts (ECMWF). Twelve atmospheric and surface fields were derived from this archive: altitude, surface (screen level) air temperature and specific humidity, integrated water vapor, rain rate, etc.

The 3-D fields, together with the available information on rain and clouds, were processed by the Earth Vegetation Atmosphere (EVA) model proposed by Kerr and Njoku (1990), and global estimates of τ and T_{ATMeq} were obtained. A statistical analysis was performed to underscore the influence of each of the twelve fields on τ_{ATM} and T_{ATMeq}. The most explicative fields for optical thickness τ_{ATM} were found to be surface altitude (Z) and surface temperature (T_{2m}) with values of square correlation coefficient R^2 of 82 and 17 %, respectively. It was found that the other fields have a much lower effects on τ_{ATM}. The equivalent atmospheric temperature, T_{ATMeq}, is strongly related to the surface air temperature (R^2=95.7 %) and less to the water content of the atmosphere ($R^2 \sim 60$ %).

In order to quantify the influence of water on the atmospheric absorption at L-band, τ_{ATM} and T_{ATMeq} were computed as previously but the water content of the atmosphere was forced to be equal to zero (this case is referred to as dry conditions). Z and T_{2m} were relevant to explain the variations of the obtained values of τ_{ATM} and T_{ATMe} in dry conditions. A simple, statistical parameterization of τ_{ATM} and T_{ATMeq} that used only the surface altitude, Z, and surface temperature, T_{2m}, that accounted respectively for oxygen absorption and air temperature T_{2m} was obtained:

$$\tau_{ATM} = \exp[-3.9262 - 0.2211\,\mathbf{Z}(\text{km}) - 0.00369\,\mathbf{T_{2m}}(\text{K})] \qquad (9)$$

$$T_{ATMeq} = \exp[4.9274 + 0.002195\,\mathbf{T_{2m}}(\text{K})] \qquad (10)$$

Despite the fact that the water content of atmosphere is ignored in (9) and (10), the rms error resulting from the use of these equations in order to estimate the down-welling atmospheric emission $Tb_{SKY\text{-}D}$ at nadir is only 0.06 K with a mean bias of –0.03 K.

8. Global half-degree maps of synthetic L-band brightness temperatures

Global half-degree maps of synthetic L-band T_B were simulated with L-MEB at 0600 and 1800 LST, each day, from January 1, 1987 to December 31, 1988, for incidence angles of 0 , 20 , 30 , 40 , and 50°, at vertical and horizontal polarizations (V and H, respectively). T_B values ranged between about 140 and 300 K. To illustrate the obtained global synthetic data set, the annual amplitude of T_B and polarization difference D_P is presented in Fig. 2. The L-band T_B observations are unlikely to be useful over regions where the annual amplitude of both T_B and D_P are small. This occurred mainly over rainforests in Africa and South America. Conversely, very large amplitude could be seen over desertic areas (Sahara, Arabic Peninsula, centre of Australia etc.) where T_B is strongly sensitive to soil moisture, and in areas dominated by crops (Western part of Europe, centre of the USA, South-eastern part of China, etc.) where T_B is strongly sensitive to both soil moisture and to the vegetation development. Over boreal forests, there is a low amplitude in the polarization difference D_P, but the seasonal change in the L-band emission is significant. These global daily maps have been used in two studies to develop and evaluate methods to retrieve soil moisture from near-future L-band space

mission using statistical (Pellarin et al., 2003b) or forward model inversion (Pellarin et al., 2003c) methods.

Insert Fig. 3

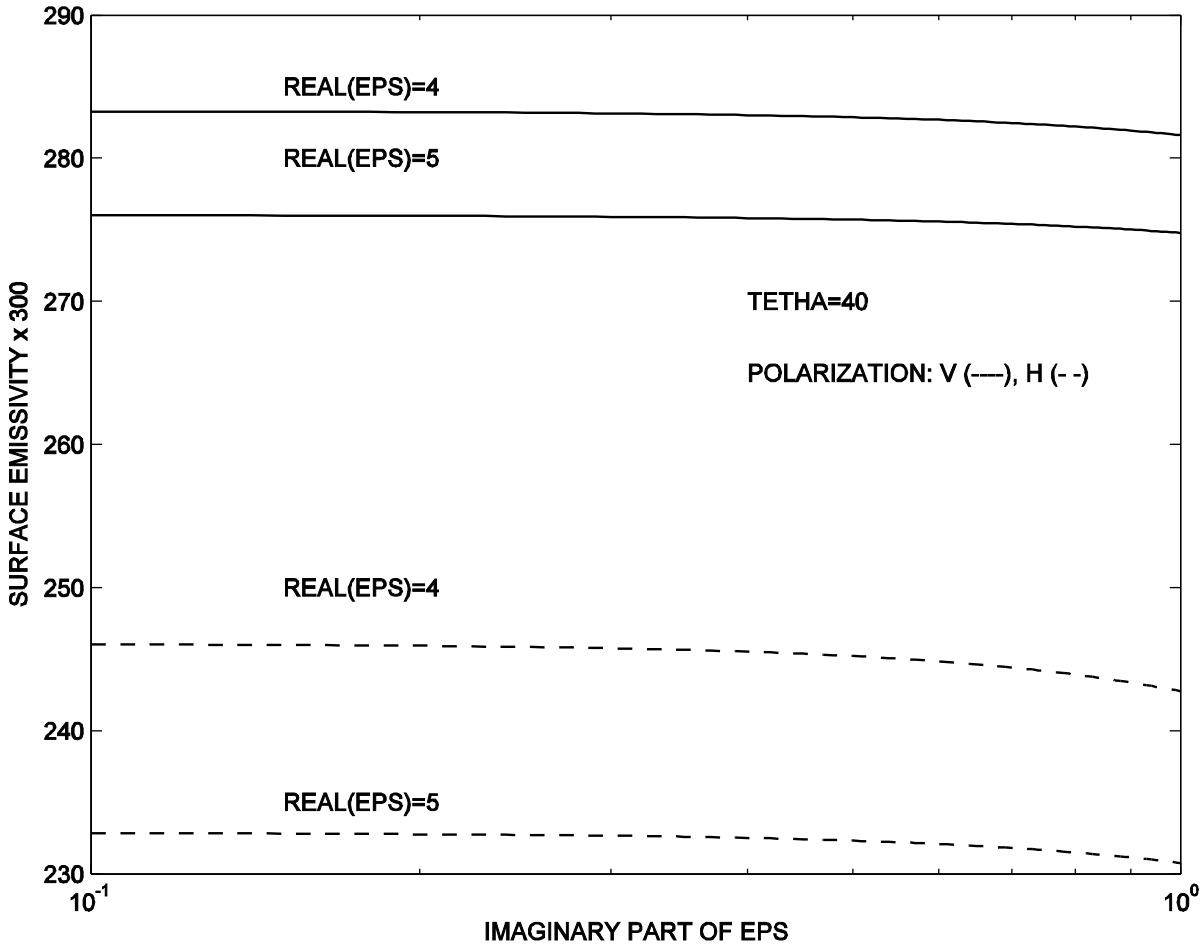

Fig. 1. Sensitivity of the emissivity to the real and imaginary part of the frozen soil dielectric constant.

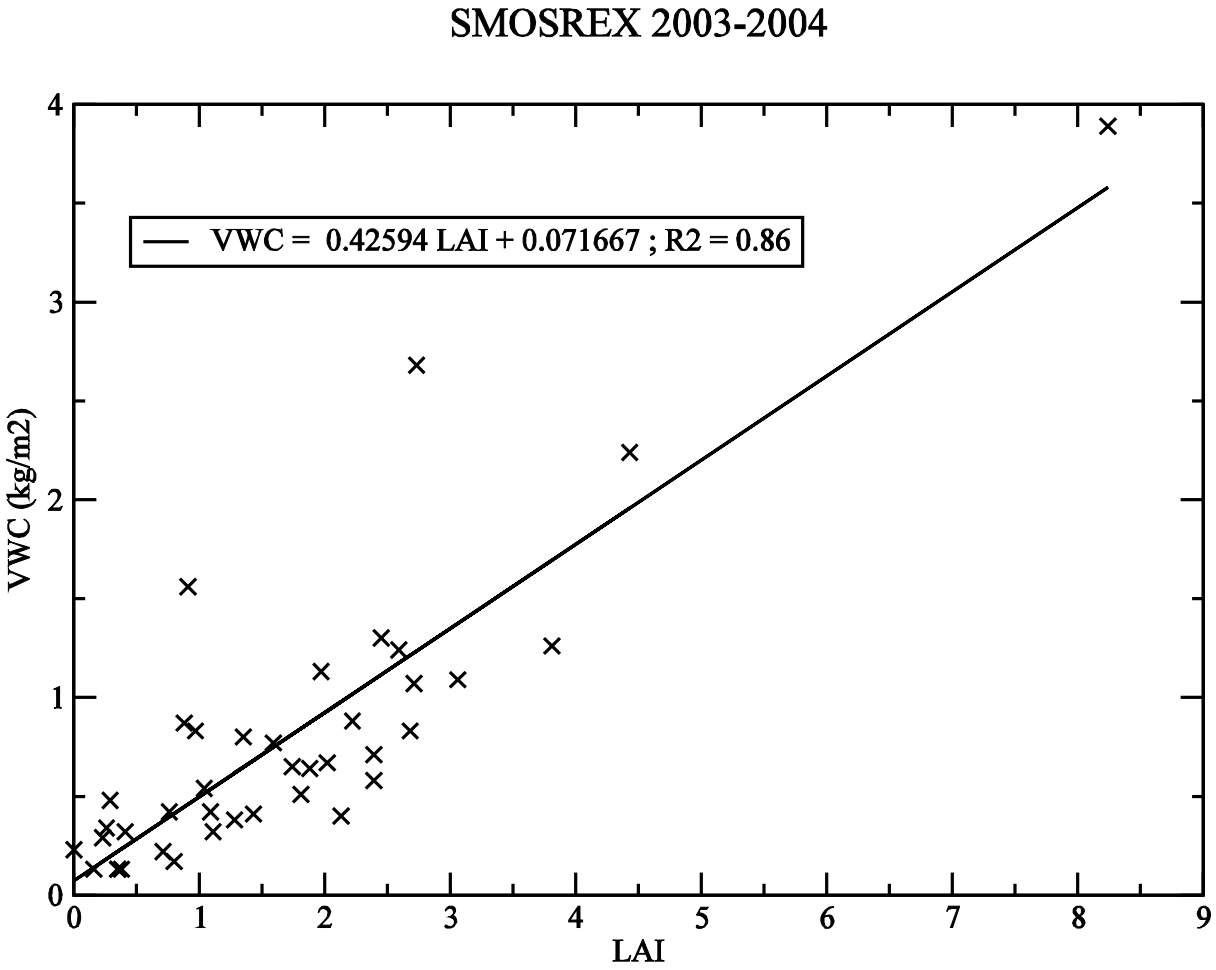

Fig 2. Relationship between Leaf Area Index (LAI) and the vegetation water content (VWC, kg/m^2) over a fallow (SMOSREX experiment, 2003-2004).

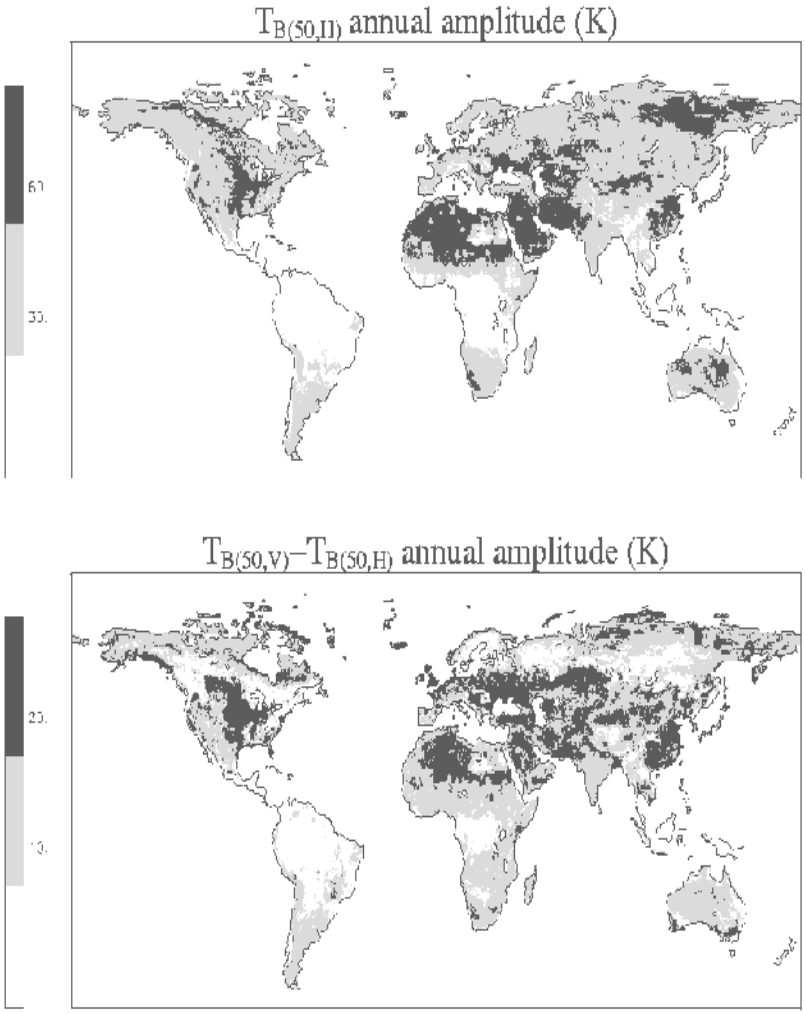

Fig 3. Global half-degree maps of the annual amplitude of (top) the synthetic L-band H-polarized brightness temperatures, and (bottom) the polarization difference, at an incidence angle of 50°, for 1988 at 0600 LST. The three considered classes correspond to (top) 0–30 K, 30–60 K, more than 60 K, and (bottom) 0–10 K, 10–20 K, more than 20 K (Pellarin et al., 2003a; reproduced by permission of IEEE, ©2003)